

Electronic Supplementary Information for
Improved Polymerization and Depolymerization Kinetics of
Poly(ethylene Terephthalate) by Co-polymerization with 2,5-
Furandicarboxylic Acid

Anup S. Joshi^{a,b}, Niloofar Alipourasiabi^{a,b}, Keerthi Vinnakota^{a,b}, Maria R. Coleman^{a,b}, Joseph G.
Lawrence^{a,b}

^a Department of Chemical Engineering, University of Toledo, OH 43606, USA

^b Polymer Institute, University of Toledo, OH 43606, USA

¹H NMR spectroscopy results after paste making step

During the commercial synthesis of PET by direct esterification, the paste making step is used to homogenize the monomers and make a slurry of TPA in EG prior to introducing the reactants into the esterification reactor.¹ A similar paste making step was carried out prior to the coesterification of TPA and FDCA with EG. ¹H NMR spectra were recorded to ensure that the temperature used for paste making step did not initiate the esterification reaction of TPA and FDCA with EG interfering with the kinetics data. Figure S-1(a) shows the ¹H NMR spectra for PET, PETF10, and PETF20 samples after the paste making step at 100 °C for 25 minutes. Peaks corresponding to free EG, FDCA, and TPA are tabulated in Table S-1. Figure S-1(b) shows the region corresponding to the oxyethylene protons of ethylene glycol. Even though a minute amount of esterified products can be observed in the zoomed in spectra at 3.70 and 4.30 ppm, the

conversion values calculated based on the area under these peaks (more details in the next section) compared to the free EG peak were statistically insignificant. Therefore, the NMR spectra confirmed that the temperature and time used for paste making step of the reaction protocol was insufficient to initiate the esterification reaction of FDCA and TPA with EG.

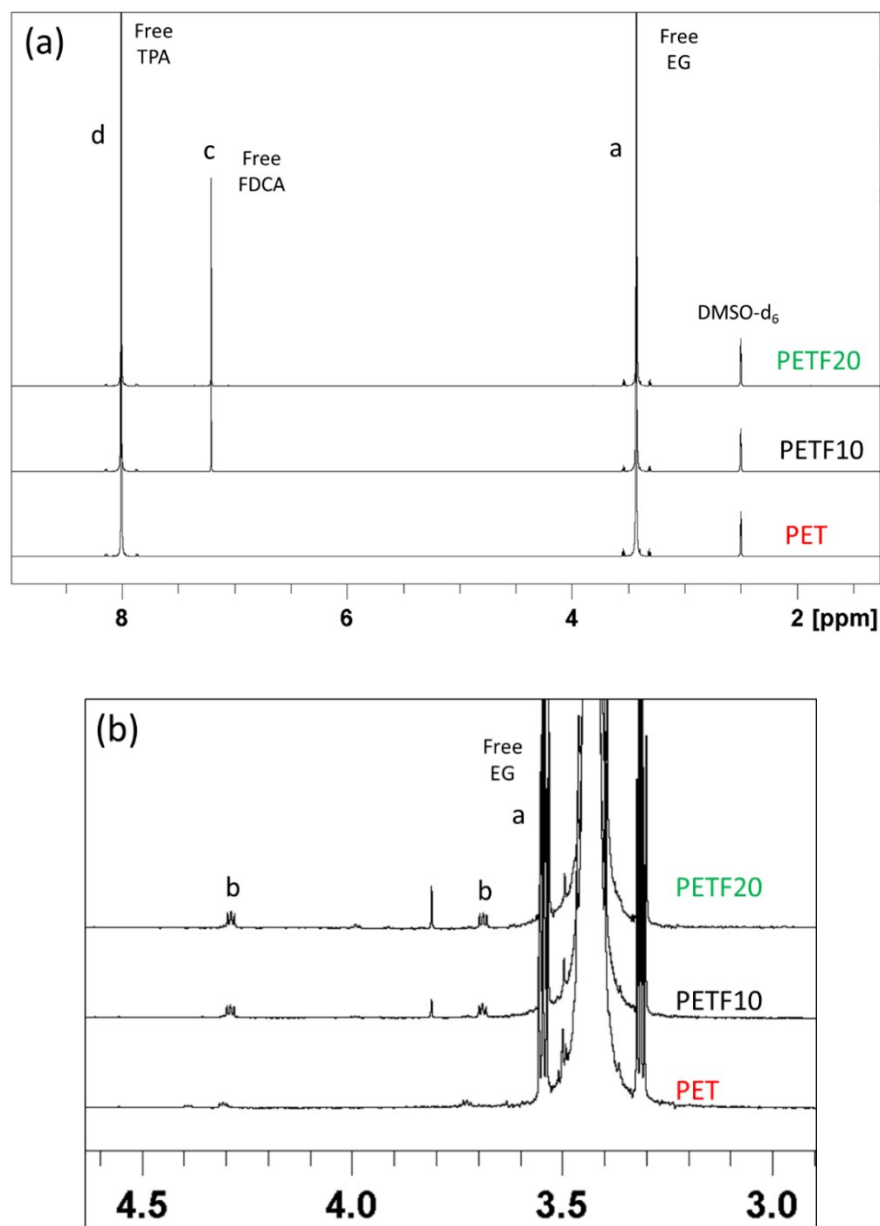


Figure S-1: (a) ¹H NMR spectra for PET, PETF10 and PETF20 samples after the paste making step. (b) region corresponding to the oxyethylene protons from EG

Table S-1: Peak assignment of protons from ^1H NMR spectra shown in Figure S-1

Peak	Chemical shift (ppm)	Assignment
a	3.41	Oxyethylene protons of free EG
b	3.70 and 4.30	Oxyethylene protons from EG end group
c	7.25	Aromatic protons of free FDCA
d	8.02	Aromatic protons of free TPA

Carboxyl and Hydroxyl end group conversion using ^1H and ^{13}C NMR spectroscopy

NMR spectroscopy has been previously used to determine conversions of TPA and EG end groups for the esterification step.² This method was extended to determine the end group conversion of FDCA due to the structural similarity between the two diacids.³ Figure S-2 describes the ^1H and ^{13}C chemical shift assignment for different chemical species involved during the esterification reaction.

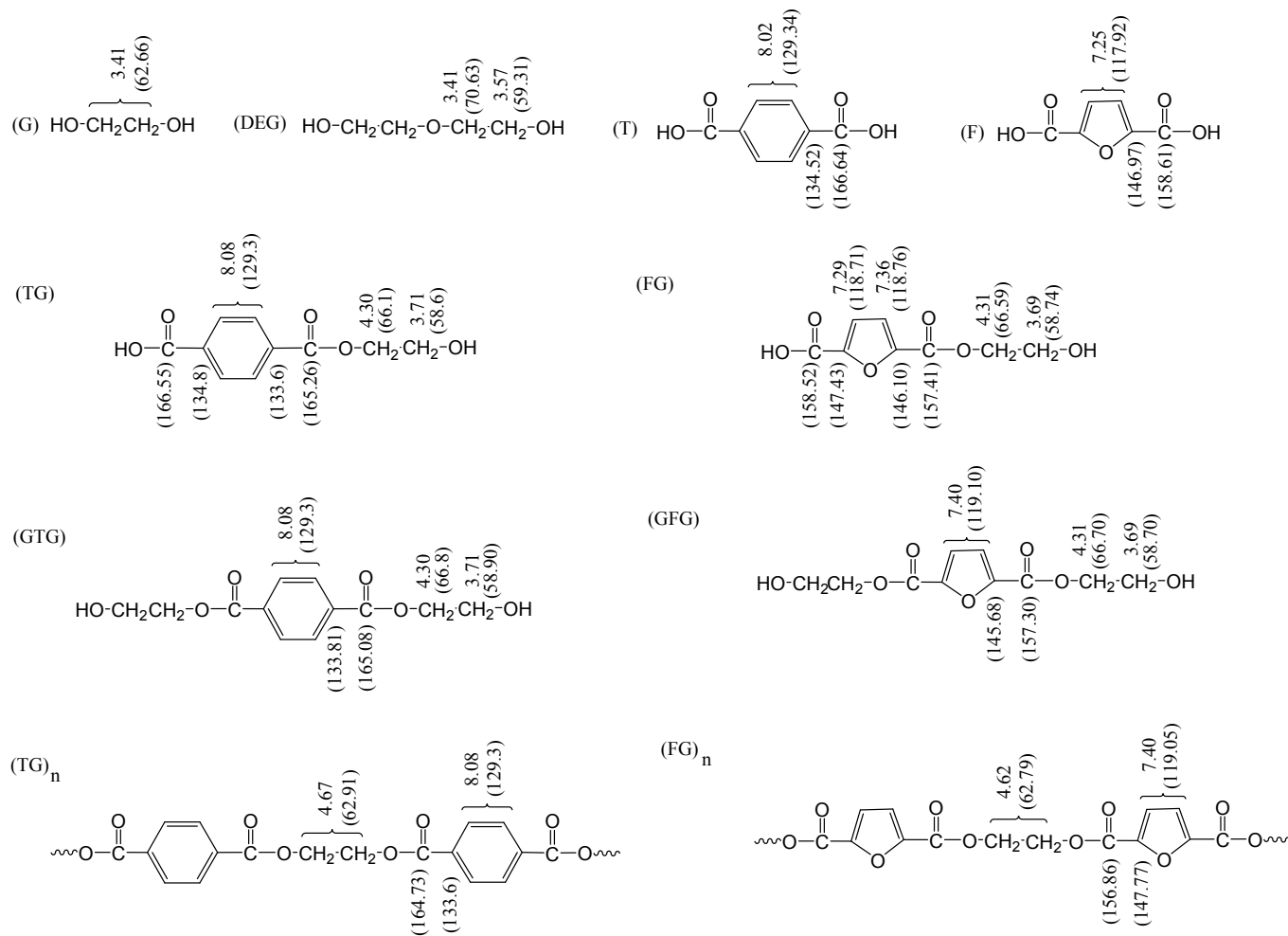


Figure S-2: ^1H and ^{13}C (in brackets) NMR peak assignments for (G) ethylene glycol, (DEG) diethylene glycol, (T) terephthalic acid, (F) 2,5-furandicarboxylic acid, (TG) hydroxyethyl terephthalate, (FG) hydroxyethyl furandicarboxylate, (GTG) bishydroxyethyl terephthalate/BHET, (GFG) bishydroxyethyl furandicarboxylate/BHEF, (TG)_n polyethylene terephthalate/PET and (FG)_n polyethylene furandicarboxylate/PEF

Hydroxyl end group conversion by ¹H NMR

Oxyethylene proton resonances arising from ethylene glycol residues can be used for to determine the hydroxyl end group conversion.² As shown in Figure S-3, oxyethylene protons of free EG showed a resonance peak at 3.41 ppm. As the reaction progressed, these protons showed a chemical shift because of the change in the chemical environment due to the presence of ester bond. EG present as an end group showed two peaks of the same intensity around 3.7 and 4.3 ppm. On the other hand, EG present in chain showed one peak in the range of 4.62 - 4.67 ppm downfield of the other EG resonances. This chemical shift of the oxyethylene protons due to presence of ester linkage was used to track kinetics of hydroxyl end group conversion. Based on the area under curve (AUC) of the oxyethylene peaks, hydroxyl end group conversion (X_{OH}) was determined as follows

$$\text{Hydroxyl end group conversion } (X_{OH}) = \frac{AUC(c) + 0.5 * AUC(b)}{AUC[(a) + (b) + (c)]}$$

$$\text{Mole \% of hydroxyl groups as DEG in chain} = \frac{100 * 0.5 * AUC(e)}{AUC[(a) + (b) + (c) + 0.5 * (d) + 0.5 * (e)]}$$

$$\text{Mole \% of hydroxyl groups as free DEG} = \frac{100 * 0.5 * AUC(d)}{AUC[(a) + (b) + (c) + 0.5 * (d) + 0.5 * (e)]}$$

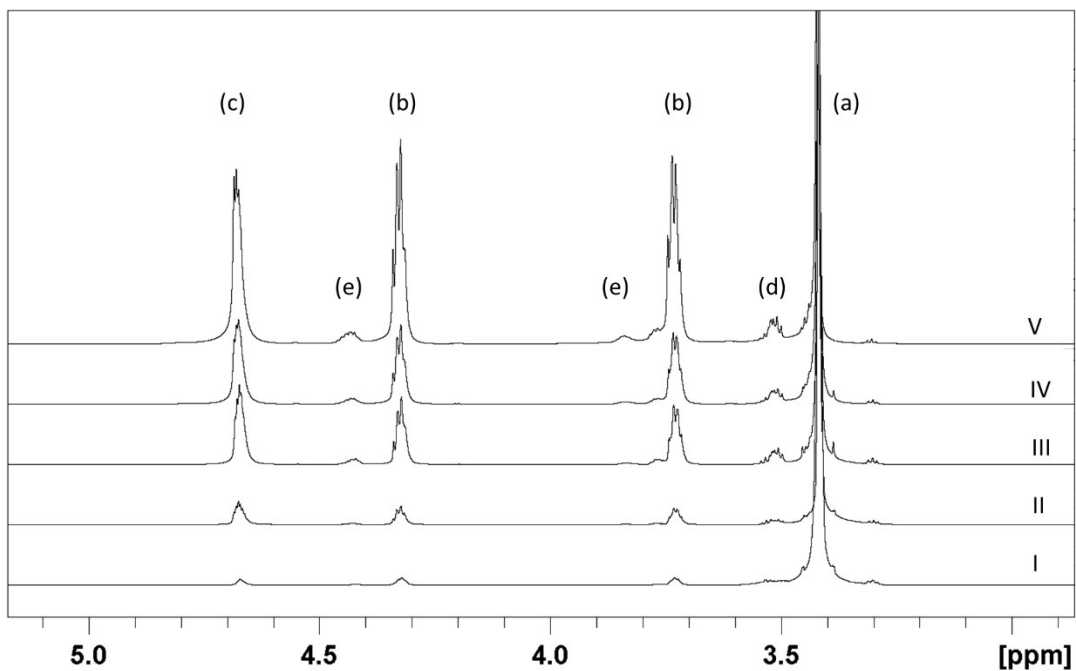


Figure S-3: ^1H NMR spectra indicating chemical shift of oxyethylene protons for free EG (a), EG present as an end group (b), EG incorporated in the polyester backbone (c), free DEG (d), and DEG incorporated in the polyester backbone (e); after (I) 0 minutes, (II) 5 minutes, (III) 10 minutes, (IV) 15 minutes, and (V) 30 minutes of esterification reaction of TPA with EG at 250 $^{\circ}\text{C}$.

Degree of randomness analysis using ¹H NMR

In the case of PETF copolymers, the peak corresponding to the oxyethylene protons in the polyester backbone (peak (c) from Figure S-3) shows splitting based on the dyad sequence as shown in Figure S-4. The area under each of the peaks identified in Figure S-4 can be used to determine dyad fractions f_{TT} , f_{TF} , f_{FT} and f_{FF} . Degree of randomness (R) and average sequence lengths of PET (L_{nT}) and PEF (L_{nF}) blocks can be calculated as follows^{4,5}

$$R = P_{FT} + P_{TF}$$

$$P_{FT} = \frac{\frac{f_{FT} + f_{TF}}{2}}{\frac{f_{FT} + f_{TF}}{2} + f_{FF}} = \frac{1}{L_{nF}}$$

$$P_{TF} = \frac{\frac{f_{FT} + f_{TF}}{2}}{\frac{f_{FT} + f_{TF}}{2} + f_{TT}} = \frac{1}{L_{nT}}$$

Where P_{FT} and P_{TF} are the probabilities of finding PEF unit next to PET unit and PET unit next to PEF unit respectively. The calculated value of R should be equal to 1 for random copolymers, equal to 2 for alternating copolymers, and zero for block copolymers.

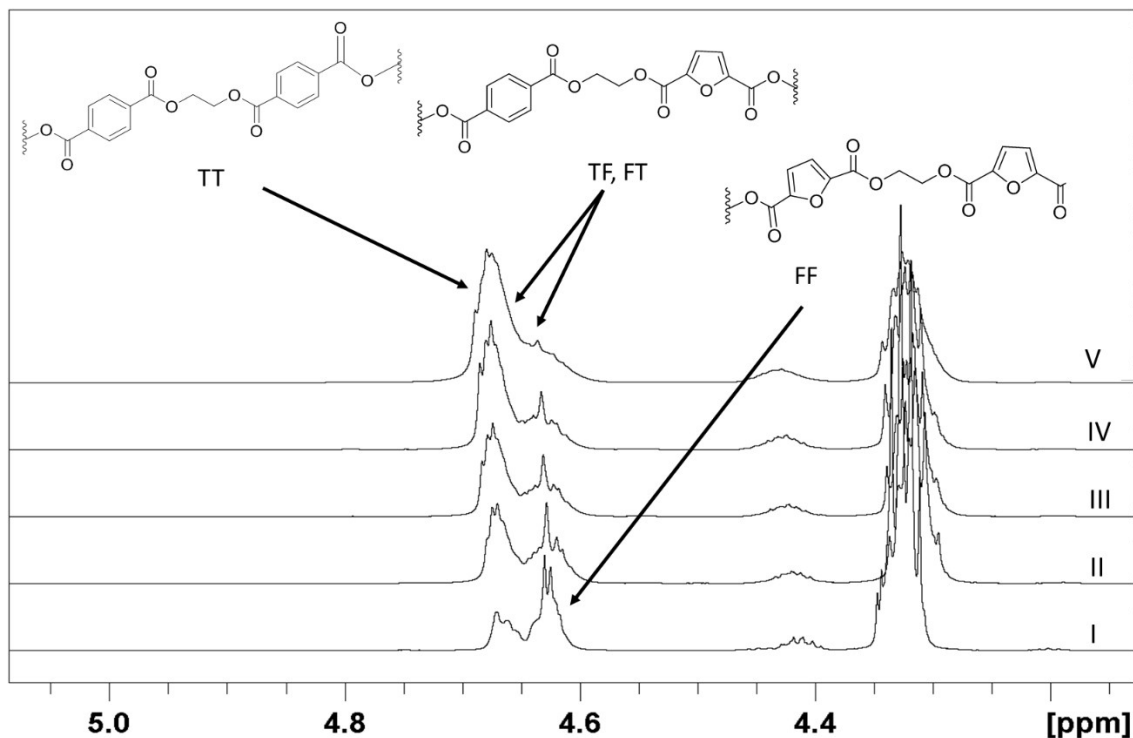


Figure S-4: ^1H NMR spectra indicating the splitting of oxyethylene protons of EG residue in the backbone depending on the dyad sequence for PETF20 sample after (I) 0 minutes, (II) 5 minutes, (III) 10 minutes, (IV) 15 minutes, and (V) 30 minutes of esterification reaction at 250 °C.

Carboxyl end group conversions using ^{13}C NMR

^{13}C resonances arising from carbonyl carbons of TPA and FDCA diacids are sensitive to their chemical environment and show chemical shift depending on the esterification of one or both carbonyls. This chemical shift of peaks can be used to determine carboxyl end group conversion of TPA end groups.² This method can also be extended to determine carboxyl end conversion for FDCA end groups.³ These methods were used to study the TPA and FDCA carboxyl end group conversion separately for a better understanding of competitive esterification kinetics. Chemical

shift of carbonyl carbons of TPA and FDCA as a function of reaction time is shown in Figure S-5 and Figure S-6.

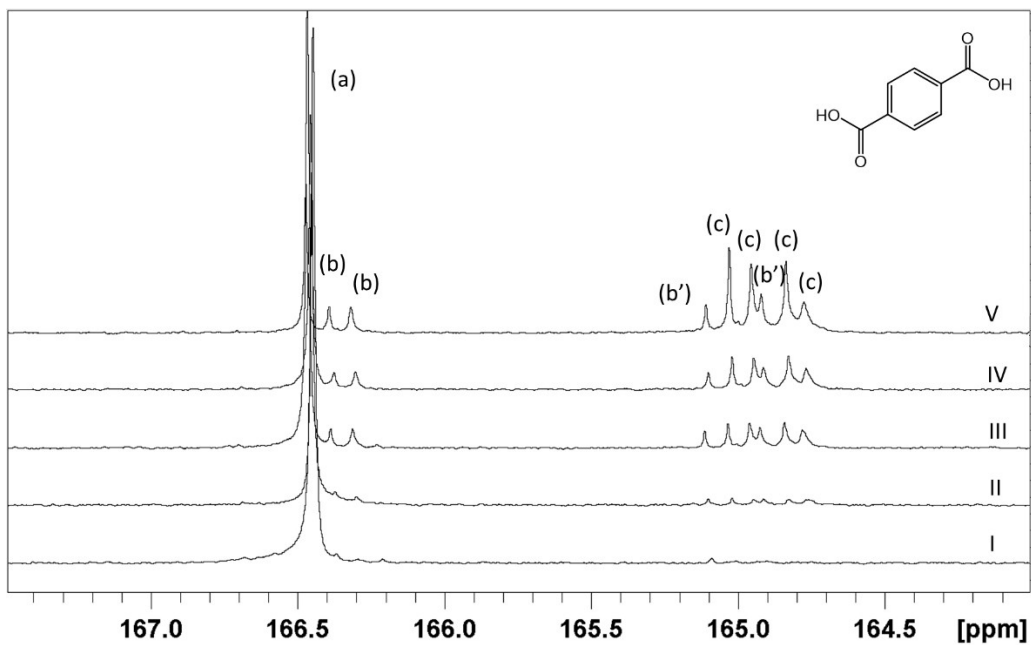


Figure S-5: ^{13}C NMR spectra indicating chemical shift of carbonyl carbon for free TPA (a), TPA present as an end group (b, b') and TPA incorporated in polyester backbone (c) after (I) 0 minutes, (II) 5 minutes, (III) 10 minutes, (IV) 15 minutes, and (V) 30 minutes of esterification reaction of TPA with EG at 250 °C.

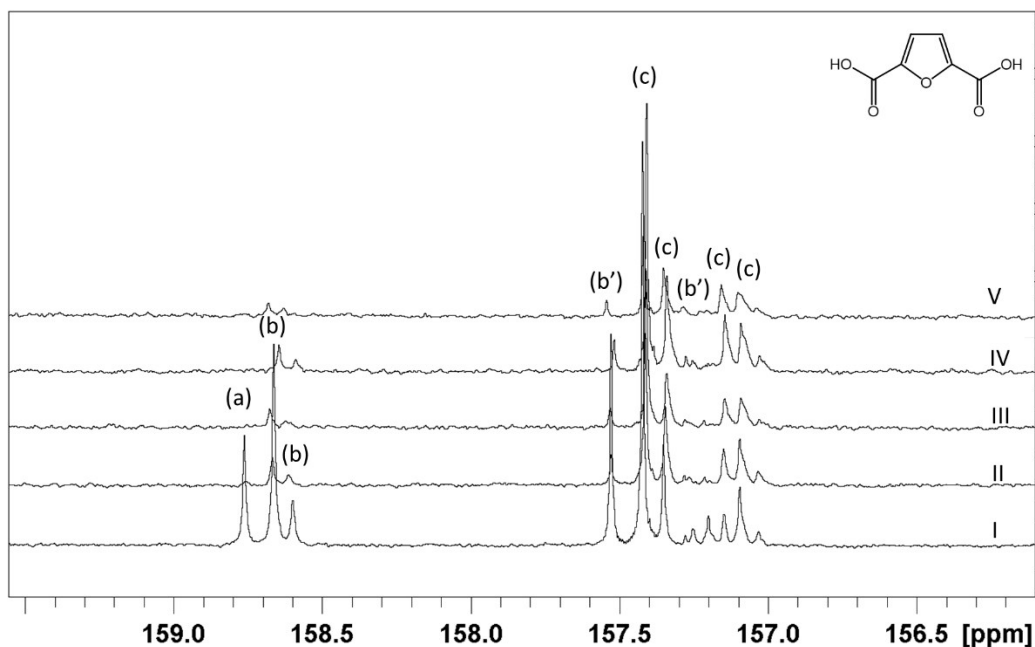


Figure S-6: ^{13}C NMR spectra indicating chemical shift of carbonyl carbon for free FDCA (a), FDCA present as an end group (b, b') and FDCA incorporated in polyester backbone (c) after (I) 0 minutes, (II) 5 minutes, (III) 10 minutes, (IV) 15 minutes, and (V) 30 minutes of esterification reaction of PETF20 at 250 °C.

Based on the area under curve (AUC) of the carbonyl carbon peaks, acid end group conversion for TPA ($X_{\text{COOH, TPA}}$) and FDCA ($X_{\text{COOH, FDCA}}$) was determined using this formula

$$\text{Carboxyl end group conversion } (X_{\text{COOH, TPA}} \text{ or } X_{\text{COOH, FDCA}}) = \frac{\text{AUC}[(c) + (b')]}{\text{AUC}[(a) + (b) + (b') + (c)]}$$

Molecular weight evolution by MALDI-MS

MALDI-ToF-MS spectra show peak corresponding to the molecular mass/charge (m/e) of the polymer chain with the intensity of the peak being proportional to the population of the chains with the corresponding m/e. The polymer chains are ionized during the detection processes and often show sodiated or protonated masses (ionized complex with sodium or proton) due to the sodium or hydrogen ions present in the detectors.⁶

Figure S-8 and Figure S-9 show the MALDI-MS spectra obtained for PETF copolyester samples at each reaction temperature. Following the incorporation of furan units, series of new peaks with a difference of 10 Daltons can be seen in the MALDI spectra. For example, the peak at 1237 Daltons in the PET spectrum corresponds to the sodium salt of hexamer of PET as shown in Figure S-7. (6 X 192 (repeat unit mass) + 62 (EG end group) + 23 (Sodium mass) = 1237). With replacement of one or more TPA units (repeat unit MW = 192) in the hexamer with the FDCA units (repeat unit MW = 182) results in the new peaks with 10 Dalton difference. All such peaks were considered in the calculation of the number average molecular weight.

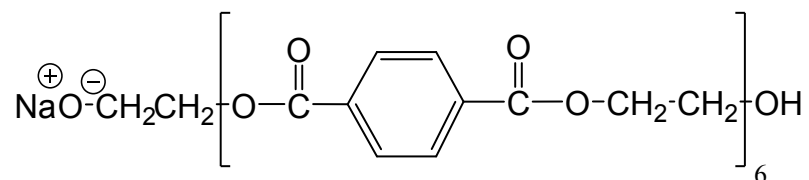


Figure S-7: Hexamer of PET with hydroxyl end groups in the sodium salt form

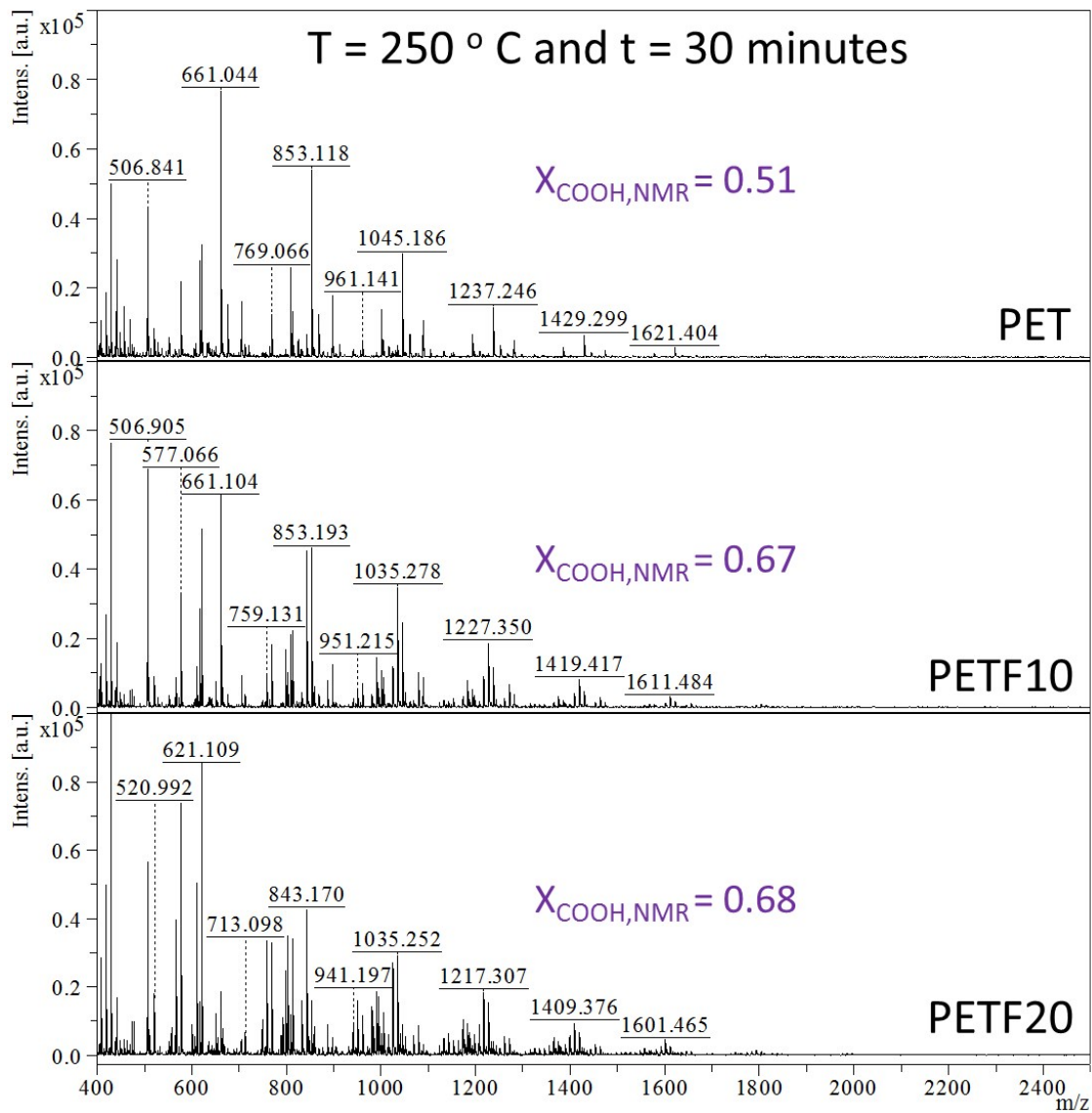


Figure S-8: MALDI-MS spectra of PET, PETF10, and PETF20 at T = 250 °C and t = 30 minutes with corresponding X_{COOH,Total} values calculated by NMR

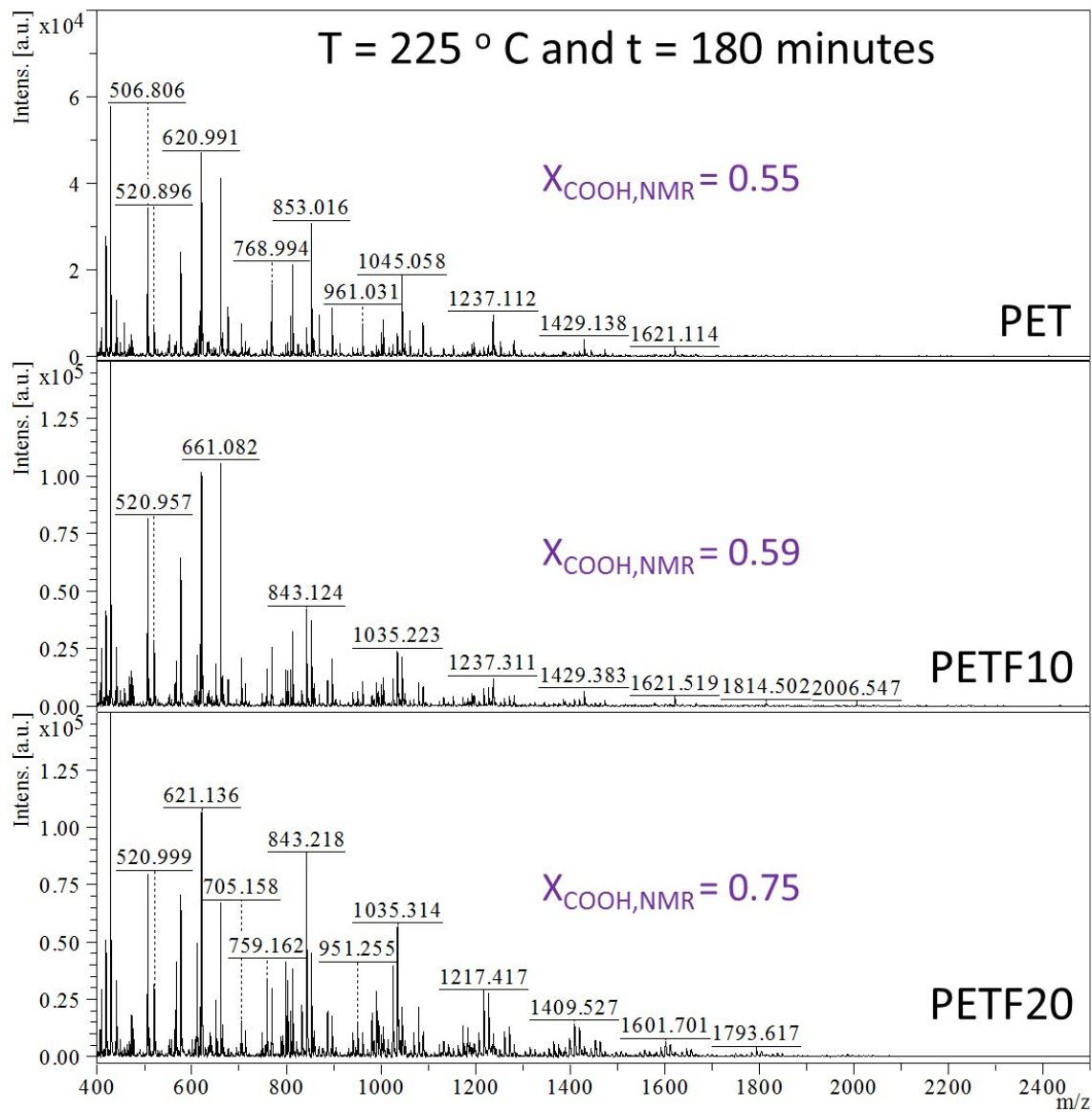


Figure S-9: MALDI-MS spectra of PET, PETF10 and PETF20 at T = 225 °C and t = 180 minutes with corresponding $X_{\text{COOH,Total}}$ values calculated by NMR

The PEF oligomers used for solubility studies were analyzed for molecular weight using MALDI-MS. The sample had a number average molecular weight of 930 Daltons and a degree of polymerization of 5 as shown below.

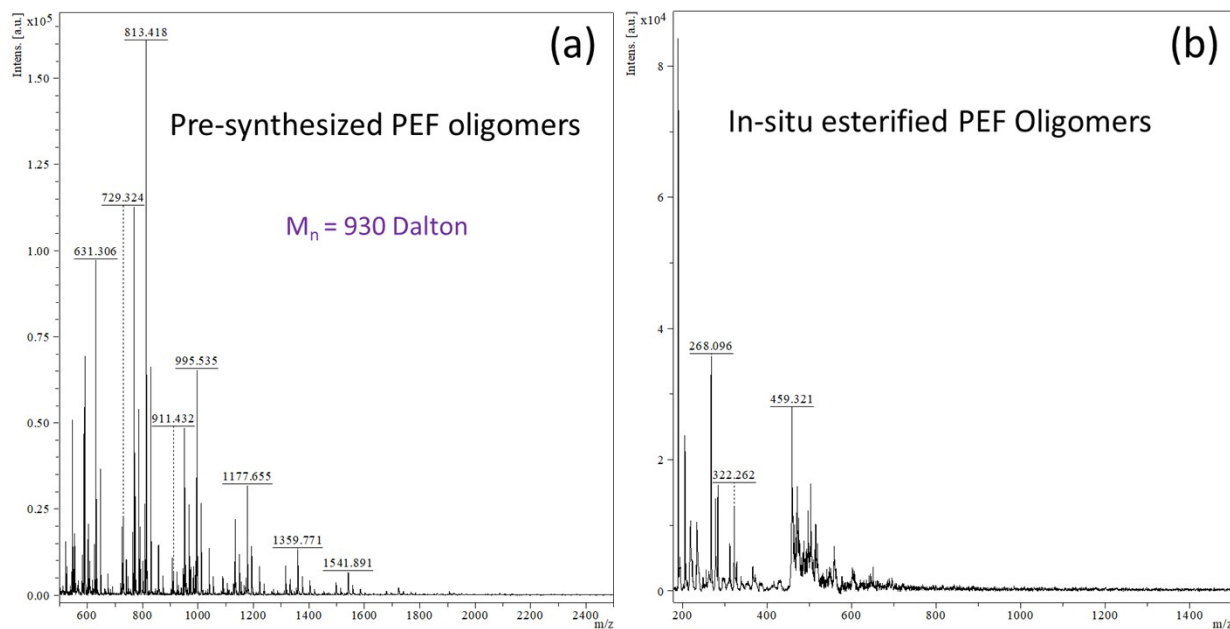


Figure S-10: MALDI-MS spectra of (a) pre-synthesized PEF oligomer used for solubility studies and (b) in-situ esterified PEF oligomers for TPA with FDCA sample showing clear point at $T =$

180 °C

Solubility parameter calculation using Hoftyzer and Van Krevelen method ⁷

The solubility parameter for the monomers and oligomers was calculated using the group contribution method developed by Hoftyzer and Van Krevelen.⁷ The overall solubility parameter (δ) is divided into three components based on the structural contributions as (i) dispersive force component (δ_d), (ii) polar force component (δ_p), and (iii) hydrogen bonding component (δ_h). Each component can be calculated by functional group contribution to (i) F_d , dispersive contribution to the molar attraction constant, (ii) F_p , polar contribution to the molar attraction constant, and (iii) E_h , the hydrogen bonding contribution to the cohesive energy using equations below.

$$\text{Dispersive contribution to solubility parameter: } \delta_d = \frac{\Sigma F_{di}}{V}$$

$$\text{Polar contribution to solubility parameter: } \delta_p = \frac{\sqrt{\Sigma F_{pi}^2}}{V} * \text{symmetry factor}$$

$$\text{Hydrogen bonding contribution to solubility parameter: } \delta_h = \sqrt{\frac{\Sigma E_{hi}}{V}}$$

Where V is the molar volume (cm³/mol). The symmetry factor is 0.5 for one plane of symmetry, 0.25 for two planes of symmetry, and 0 for more planes of symmetry.

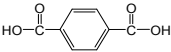
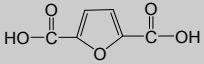
The overall solubility parameter (δ) can be calculated from the contributions by

$$\delta^2 = \delta_d^2 + \delta_p^2 + \delta_h^2$$

Table S-2 shows the calculated solubility parameters for different chemical species involved in the esterification reaction.

Table S-2: Contributions to the solubility parameter, δ (MJ/m³)^{1/2} for different species involved in the esterification reaction calculated based on group contribution method by Hoftyzer and Van

Krevelen ⁷

Species	Molar mass	Structure	δ_d	δ_p	δ_h	δ
EG	62	HO-CH ₂ CH ₂ -OH	16.5	3.0	26.2	31.1
TPA	166		21.3	1.4	13.5	25.3
FDCA	156		21.4	2.0	16.1	26.9
BHEF	244	HO-CH ₂ CH ₂ - $\left[\text{O}-\text{C}(=\text{O})-\text{furan}-\text{C}(=\text{O})-\text{O}-\text{CH}_2\text{CH}_2 \right]_1$ -OH	19.7	3.4	19.0	27.6
PEF dimer	426	HO-CH ₂ CH ₂ - $\left[\text{O}-\text{C}(=\text{O})-\text{furan}-\text{C}(=\text{O})-\text{O}-\text{CH}_2\text{CH}_2 \right]_2$ -OH	20.4	5.2	17.0	27.1
PEF trimer	608	HO-CH ₂ CH ₂ - $\left[\text{O}-\text{C}(=\text{O})-\text{furan}-\text{C}(=\text{O})-\text{O}-\text{CH}_2\text{CH}_2 \right]_3$ -OH	20.8	4.4	16.0	26.6
PEF tetramer	790	HO-CH ₂ CH ₂ - $\left[\text{O}-\text{C}(=\text{O})-\text{furan}-\text{C}(=\text{O})-\text{O}-\text{CH}_2\text{CH}_2 \right]_4$ -OH	20.9	3.8	15.4	26.2
PEF pentamer	972	HO-CH ₂ CH ₂ - $\left[\text{O}-\text{C}(=\text{O})-\text{furan}-\text{C}(=\text{O})-\text{O}-\text{CH}_2\text{CH}_2 \right]_5$ -OH	21.0	3.5	15.0	26.0

Effect of copolymerization on diethylene glycol production

Diethylene glycol (DEG) formation is a reported side reaction during the esterification step of PET synthesis.⁸ The DEG content in the polyester backbone must be regulated since DEG can plasticize the polymer and reduce the T_g in addition to increasing the susceptibility to hydrolytic degradation.⁹ The etherification reaction of EG to produce DEG is acid-catalyzed.⁸ Lower pKa of FDCA was expected to accelerate the DEG formation reaction. Higher values of DEG in the case of PEF synthesis have been reported before.³ To understand the effect of copolymerization on DEG production, ^1H NMR spectra were used to determine the amount of DEG produced and reacted with the polymer as shown in the NMR section above. Figure S-11(a) and (b) show the effect of copolymerization on DEG incorporated in the polymer chain. As expected, the presence of FDCA and esterified FDCA products accelerated the DEG formation reaction and resulted in higher amounts of DEG in the polymer chains. Please note that no DEG suppressor was added to the reaction mixture to moderate the pH of the reaction media. At lower temperature of 225 °C, the DEG formation was much slower and the effect of copolymerization on DEG production was relatively small. Figure S-12(a) and (b) show the free DEG present in the reaction mixture as a function of the reaction time. In general, the amount of free DEG production was reached a constant value after higher reaction times. The increase in DEG production due to the presence of FDCA was much less pronounced at 225 °C similar to the Figure S-11(b). Hence, it was concluded that the presence of more acidic FDCA in the reaction media accelerated the DEG production and subsequent incorporation of DEG in the growing polymer chains. At lower temperature of 225 °C, this effect was minimal due to reduced reaction kinetics.

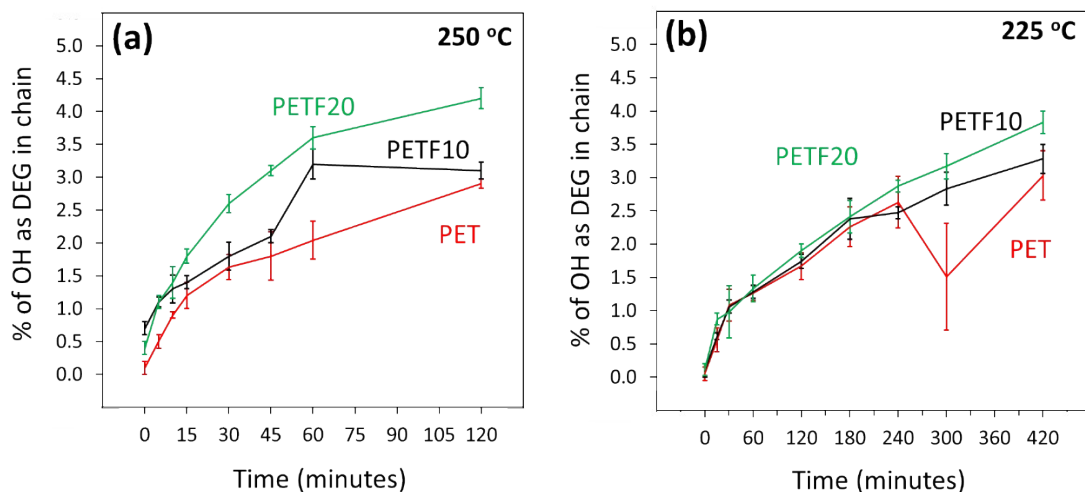


Figure S-11: Mole % of hydroxyl end groups present as DEG in chain determined by ^1H NMR for PET (-), PETF10 (-) and PETF20 (-) for direct esterification performed at (a) 250 °C and (b) 225 °C

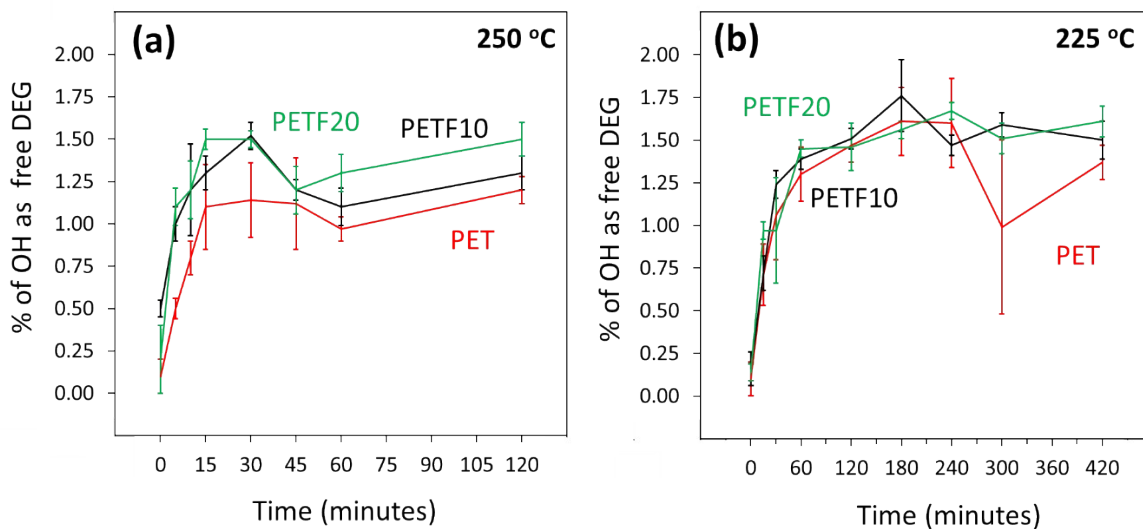


Figure S-12: Mole % of hydroxyl end groups present as free DEG determined by ^1H NMR for PET (-), PETF10 (-) and PETF20 (-) for direct esterification performed at (a) 250 °C and (b) 225 °C

¹H NMR spectrum of monomers obtained after alkaline hydrolysis of PETF20 sample

Figure S-13 shows the ¹H NMR spectrum of the recovered diacids after alkaline hydrolysis of PETF20 flake sample. Spectrum shows phenyl and furanic protons indicated by (a) and (h) respectively. The ratio of the peaks is consistent with the expected molar ratios in case of PETF20 samples. This spectrum confirms that depolymerization was complete and yielded in a good purity diacid monomers, TPA and FDCA.

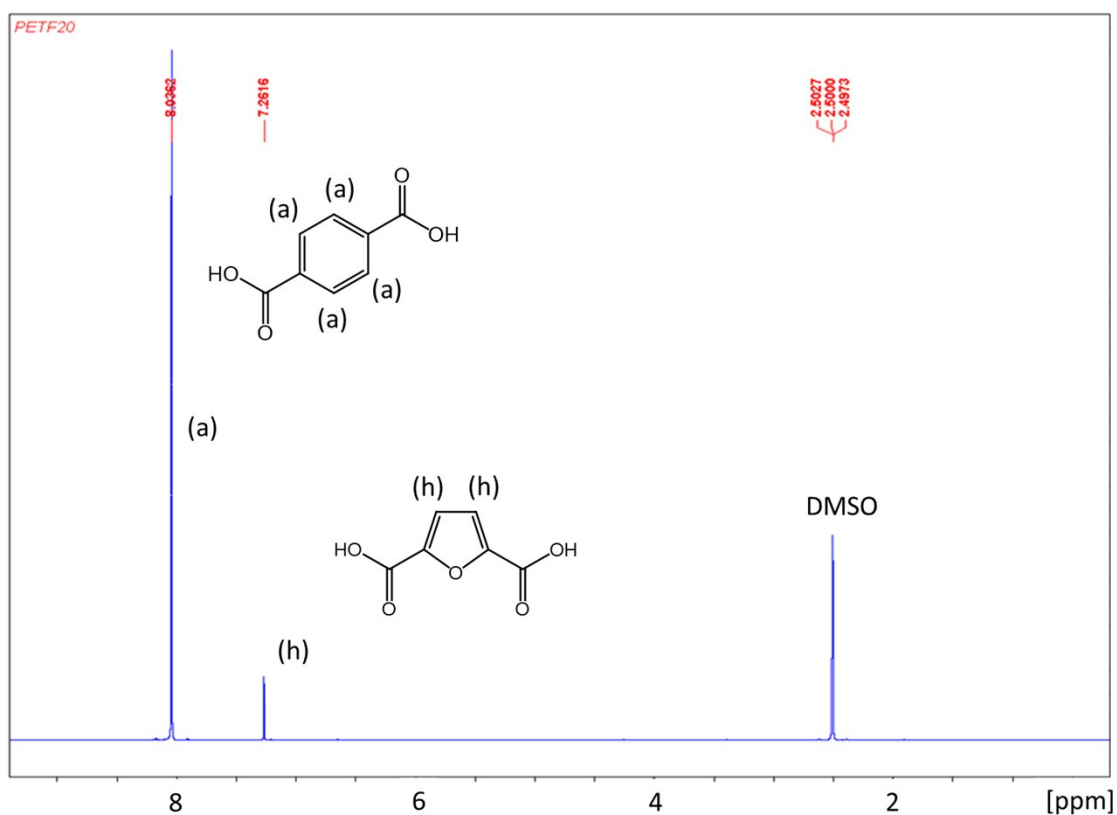


Figure S-13: ¹H NMR spectrum of recovered TPA and FDCA after alkaline hydrolysis of PETF20 flakes

REFERENCES

1. Aharoni, S. M., Industrial-Scale Production of Polyesters, Especially Poly(Ethylene Terephthalate). In *Handbook of Thermoplastic Polyesters*, Wiley-VCH Verlag GmbH & Co. KGaA: 2005; pp 59-103.
2. Pétiand, R.; Waton, H.; Pham, Q.-T., A ¹H and ¹³C n.m.r. study of the products from direct polyesterification of ethylene glycol and terephthalic acid. *Polymer* **1992**, *33* (15), 3155-3161.
3. Joshi, A. S.; Alipourasiabi, N.; Kim, Y.-W.; Coleman, M. R.; Lawrence, J. G., Role of enhanced solubility in esterification of 2,5-furandicarboxylic acid with ethylene glycol at reduced temperatures: energy efficient synthesis of poly(ethylene 2,5-furandicarboxylate). *Reaction Chemistry & Engineering* **2018**, *3* (4), 447-453.
4. Konstantopoulou, M.; Terzopoulou, Z.; Nerantzaki, M.; Tsagkalias, J.; Achilias, D. S.; Bikiaris, D. N.; Exarhopoulos, S.; Papageorgiou, D. G.; Papageorgiou, G. Z., Poly(ethylene furanoate-co-ethylene terephthalate) biobased copolymers: Synthesis, thermal properties and cocrystallization behavior. *European Polymer Journal* **2017**, *89*, 349-366.
5. Yamadera, R.; Murano, M., The determination of randomness in copolyesters by high resolution nuclear magnetic resonance. *Journal of Polymer Science Part A-1: Polymer Chemistry* **1967**, *5* (9), 2259-2268.
6. Leite, J. F.; Hajivandi, M. R.; Diller, T.; Pope, R. M., Removal of sodium and potassium adducts using a matrix additive during matrix-associated laser desorption/ionization time-of-flight mass spectrometric analysis of peptides. *Rapid communications in mass spectrometry : RCM* **2004**, *18* (23), 2953-9.
7. Van Krevelen, D. W.; Te Nijenhuis, K., Chapter 7 - Cohesive Properties and Solubility. In *Properties of Polymers (Fourth Edition)*, Elsevier: Amsterdam, 2009; pp 189-227.
8. Rieckmann, T.; Völker, S., Poly(Ethylene Terephthalate) Polymerization – Mechanism, Catalysis, Kinetics, Mass Transfer and Reactor Design. In *Modern Polyesters: Chemistry and Technology of Polyesters and Copolyesters*, John Wiley & Sons, Ltd: 2004; pp 29-115.
9. de Ilarduya, A. M.; Muñoz-Guerra, S., Chemical Structure and Microstructure of Poly(alkylene terephthalate)s, their Copolyesters, and their Blends as Studied by NMR. *Macromolecular Chemistry and Physics* **2014**, *215* (22), 2138-2160.